2024 46th Annual International Conference of the IEEE Engineering in Medicine and Biology Society (EMBC) | 979-8-3503-7149-9/24/$31.00 ©2024 IEEE | DOI: 10.1109/EMBC53108.2024.10781517

# *Automated Offline Smartphone-Assisted Microfluidic Paper-Based Analytical Device for Biomarker Detection of Alzheimer's Disease*

Sixuan Duan
*School of Advanced Technology*
*Xi'an Jiaotong-Liverpool University*
Suzhou, China
sixuan.duan20@student.xjtlu.edu.cn

Ruiqi Yong
*School of Advanced Technology*
*Xi'an Jiaotong-Liverpool University*
Suzhou, China
ruiqi.yong21@student.xjtlu.edu.cn

Hang Yuan
*School of Advanced Technology*
*Xi'an Jiaotong-Liverpool University*
Suzhou, China
hang.yuan20@student.xjtlu.edu.cn

Tianyu Cai
*School of Advanced Technology*
*Xi'an Jiaotong-Liverpool University*
Suzhou, China
tianyu.cai17@alumni.xjtlu.edu.cn

Kaizhu Huang
*Department of Electrical and Computer Engineering*
*Duke Kunshan University*
Kunshan, China
kaizhu.huang@dukekunshan.edu.cn

Kai Hoettges
*Department of Electrical and Electronic Engineering*
*University of Liverpool*
Liverpool, UK
K. Hoettges@liverpool.ac.uk

Eng Gee Lim
*School of Advanced Technology*
*Xi'an Jiaotong-Liverpool University*
Suzhou, China
enggee.lim@xjtlu.edu.cn

Pengfei Song*
*School of Advanced Technology*
*Xi'an Jiaotong-Liverpool University*
Suzhou, China
pengfei.song@xjtlu.edu.cn

***Abstract*— This paper presents a smartphone-assisted microfluidic paper-based analytical device (μPAD), which was applied to detect Alzheimer's disease biomarkers, especially in resource-limited regions. This device implements deep learning (DL)-assisted offline smartphone detection, eliminating the requirement for large computing devices and cloud computing power. In addition, a smartphone-controlled rotary valve enables a fully automated colorimetric enzyme-linked immunosorbent assay (c-ELISA) on μPADs. It reduces detection errors caused by human operation and further increases the accuracy of μPAD c-ELISA. We realized a sandwich c-ELISA targeting β-amyloid peptide 1-42 (Aβ 1-42) in artificial plasma, and our device provided a detection limit of 15.07 pg/mL. We collected 750 images for the training of the DL YOLOv5 model. The training accuracy is 88.5%, which is 11.83% higher than the traditional curve-fitting result analysis method. Utilizing the YOLOv5 model with the NCNN framework facilitated offline detection directly on the smartphone. Furthermore, we developed a smartphone application to operate the experimental process, realizing user-friendly rapid sample detection.**

***Keywords—Offline smartphone-assisted detection; Microfluidic paper-based analytical device; Deep learning; Alzheimer's disease.***

## I. INTRODUCTION

Alzheimer's disease (AD) is a progressively deteriorating neurological disease without effective treatment. Early detection and timely intervention could control the progression of AD [1, 2]. Conventional AD detection methods, such as positron emission computed tomography and magnetic resonance imaging, have high detection costs and are unsuitable for large-scale detection of AD [3, 4]. Point-of-care testing (POCT) presents a viable option for the widespread detection of AD due to its excellent sensitivity, quick response to results, and cost-effectiveness. In addition, blood biomarker detection is widely used in POCT due to its low cost and ease of access [5-7]. Furthermore, recent studies have shown the viability of utilizing plasma β-amyloid peptide 1-42 (Aβ 1-42) as a biomarker for detecting AD [8, 9]. This further promotes the potential of blood biomarker testing for large-scale detection of AD.

The microfluidic paper-based analytical device (μPAD) has gained wide utilization in POCT owing to its cost-effectiveness, ease of operation, and no need for external power sources [10, 11]. Several immunoassays have been successfully developed on the μPAD, such as electrochemistry, chemiluminescent, and fluorescent immunoassays. Among them, the colorimetric enzyme-linked immunosorbent assay (c-ELISA) is the gold standard for

The authors acknowledge the financial support from the programs of the Natural Science Foundation of the Jiangsu Higher Education (22KJB460033), Jiangsu Science and Technology Programme - Young Scholar (BK20200251) and XJTLU RDF project (RDF-18-02-20, RDF-21-02-076). This work is also partially supported by the XJTLU AI University Research Centre, Jiangsu Province Engineering Research Centre of Data Science and Cognitive Computation at XJTLU, and the SIP AI innovation platform (YZCXPT2022103). The support from the State Key Laboratory for Manufacturing Systems Engineering via the open project (SKLMS2023019) and the Key Laboratory of Bionic Engineering, Ministry of Education at Jilin University (KF2023007), is also acknowledged.

Authorized licensed use limited to: Michigan State University. Downloaded on December 23,2024 at 20:18:04 UTC from IEEE Xplore. Restrictions apply.

detecting protein biomarkers in clinical samples, with analysis conducted directly based on the color change [11-14]. With the popularity of smartphones, they have been developed and used for c-ELISA result analysis. However, different types of smartphones may affect the accuracy of the analysis. In addition, c-ELISA requires many manual operations, such as multi-step reagent addition, resulting in decreased reproducibility and efficiency. Especially in resource-limited areas, there is a lack of researchers proficient in the assay process and interpretation of results. These constraints have limited the broad adoption of c-ELISA methods for POCT.

In recent years, deep learning (DL) has provided new solutions for the problem of low accuracy in smartphone detection. Through feature collection and dataset training, the sensitivity and accuracy of smartphone detection have been improved [15-18]. However, current DL-assisted smartphone detection methods often depend on bulky equipment or cloud servers for transmitting and processing data, limiting their offline applications. Typically, in underdeveloped areas or isolated mountainous regions, the absence of enough computing devices and limited internet connectivity restrict the development of smartphone-assisted biosensing. Thus, these areas urgently need offline, low-cost, rapid devices with broad detection capabilities.

In this paper, we present an innovative smartphone-assisted μPAD for AD biomarker detection. An outstanding characteristic of the μPAD is its capability to facilitate the offline detection of the smartphone, eliminating the need for extensive computing equipment and cloud data transmission. This characteristic makes it possible to detect instantly, so it is very helpful in areas with poor infrastructure. In addition, the smartphone-controlled mechanical rotation mechanism ensures a stable and automatic c-ELISA process with less manual complexity. Our smartphone-assisted μPAD has successfully been utilized in performing complex sandwich c-ELISA for detecting Aβ 1-42 samples in artificial plasma. Additionally, we prepared a dataset including 750 images for training the DL YOLOv5 model. For result analysis, the YOLOv5 model provides greater accuracy than conventional

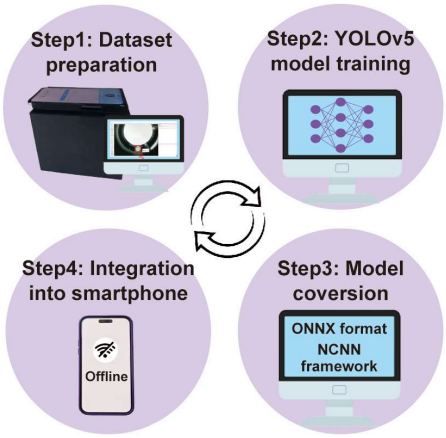


Fig. 1. The flow chart of implementing smartphone-based offline detection on μPAD.

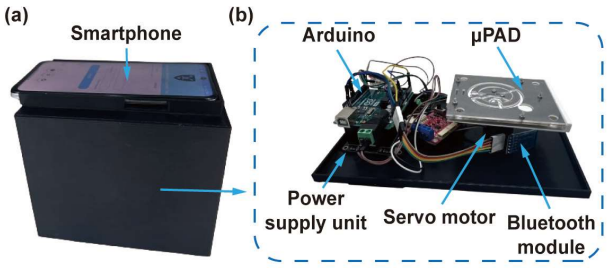


Fig. 2. (a) The photo of smartphone-assisted μPAD. (b) The photo of μPAD and other components.

curve fitting analysis approaches. Ultimately, we developed a smartphone application to operate the entire process, facilitating user-friendly and quick sample detection in offline scenarios. Our device offers an efficient method for detecting disease biomarkers.

## II. Methods

### A. Materials and reagents

Potassium periodate (>99.5%, 80106916, $KIO_4$) was purchased from Sinopharm Chemical Reagent Co., Ltd (Shanghai, China). Aβ 1-42 (bs-0107P), Aβ 1-42 antibody (bsm-41469M), horseradish peroxidase (HRP) conjugated Aβ 1-42 antibody (bsm-41470M-HRP) and 3,3',5,5'-tetramethylbenzidine (TMB) substrate solution (C04-03002) were purchased from Bioss Antibodies (Beijing, China). 10 × phosphate-buffered saline (PBS, G4207), Tween-20 (G5058), and bovine serum albumin (BSA, G5001) were purchased from Servicebio (Wuhan, China). The artificial plasma (ASP-001) was purchased from InnoReagents (Huzhou, China). The 10 × PBS was diluted using deionized (DI) water to 1 × PBS. Whatman No. 1 chromatography paper was purchased from Whatman (U.K.)

The battery module (Ywrobot), servo motor of valve driver (Feetech SCS2332), microcontroller (Arduino Uno), and Bluetooth module (HM-5), polymethyl methacrylate (PMMA) were purchased from Taobao (China).

### B. Development of offline smartphone-assisted detection

To enable smartphone-based offline detection, we first prepared a dataset by conducting sandwich c-ELISA of Aβ 1-42 samples on our μPAD. The prepared dataset was used to train the YOLOv5 model on the computer side. Then, we converted the trained YOLOv5 model into the Open Neural Network Exchange format for smartphones and deployed it to the smartphone using the Ncnn Convolutional Neural Network (NCNN) framework. Finally, an Android application was developed under the integrated development environment Android Studio (Google, U.S.A.). Fig. 1 illustrates the flow chart of implementing smartphone-based offline detection on μPAD.

### C. Fabrication of the μPAD

Figs. 2(a) and 2(b) show the photos of the smartphone-assisted μPAD and its other components. This μPAD is used

Authorized licensed use limited to: Michigan State University. Downloaded on December 23,2024 at 20:18:04 UTC from IEEE Xplore. Restrictions apply.

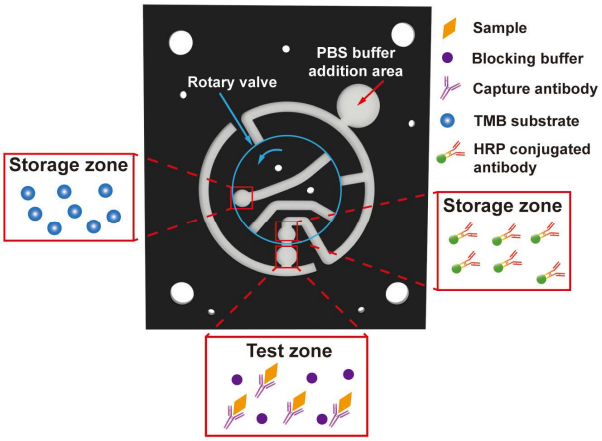


Fig. 3. The schematic diagram of the design of μPAD.

to perform sandwich c-ELISA. The smartphone is used to control the entire process with a Bluetooth module and analyze the results.

The schematic diagram of the design of μPAD is shown in Fig. 3. First, we designed the channel pattern of μPAD using AutoCAD software (Autodesk Inc., U.S.A.). The rotary valve, driven by a servo motor, is the core component of the μPAD. It contains three channels and additional storage zones at the bottom of the channels at both ends. Besides the rotary valve, the remaining part of the μPAD includes a buffer addition area, a reagent transfer channel, and a drainage channel. Additionally, we designed an overlap area of 2 mm to ensure smooth passage of the fluid through the rotary valve and its corresponding μPAD. Second, we used a wax printer (Xerox 8580DN) to print the designed pattern on Whatman No. 1 chromatography paper. Next, the paper was cut by a laser cutting machine (Han's Yueming, CMA0604-B-A) according to the printed pattern. The cut μPAD was heated on a hot plate (Cole-Parmer) at 150 °C for 60 seconds to melt the wax on the paper completely. Finally, the paper was sandwiched between two PMMA sheets and fixedly mounted with screws.

All required reagents (TMB substrate, HRP-conjugated Aβ 1-42 antibody and Aβ 1-42 antibody) are pre-stored in two storage zones and a test zone in order to perform a sandwich c-ELISA for Aβ 1-42 protein in artificial plasma samples. These zones are interconnected by the middle rotary valve. Moreover, to improve the binding properties of the test zone to the protein, we biofunctionalized the test zone with $KIO_4$ [5]. Specifically, the test zone was heated at 65 °C hot plate and 1.5 μL of aqueous $KIO_4$ (0.031 M, pH=5) was added dropwise for 20 times. Afterward, 4 μL of DI water was added to wash away the residual oxides, and the washing process was repeated twice. Finally, the paper was dried in a desiccator for at least 12 hours before use.

### *D. Construction of training datasets*

For constructing the dataset to train the DL YOLOv5 model, we generated 30 artificial plasma samples containing random concentrations of Aβ 1-42 peptide. Among these, 15 samples represented healthy, while the remaining 15 samples represented unhealthy. This method aims to consider the

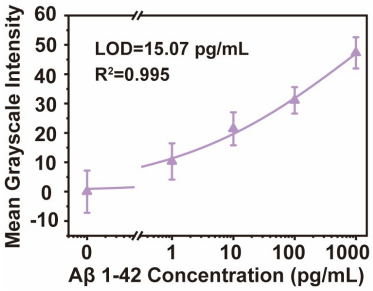


Fig. 4. The calibration curve of sandwich c-ELSIA detection.

complexity and variability of clinical samples. Several studies have utilized artificial samples to confirm the viability of their experimental methods [19, 20]. Initially, we introduce a 3 μL artificial plasma sample into the test zone for sandwich c-ELISA detection. 200 μL of 1 × PBS buffer is added to the buffer addition area of the μPAD after drying for 2 minutes. Afterwards, the Aβ 1-42 peptide in the sample is bound by the HRP-conjugated Aβ 1-42 antibody. Through the control of the rotary valve, the storage zone is then separated from the test zone after a 5-minute connection time to facilitate drying and incubation. Then, unbound antibodies are washed by the washing buffer. After 5 minutes of incubation, the TMB substrate encourages the reaction to form a blue precipitate. All the storage zones are connected to the test zone by the paper rotary valve. Each sample was repeated five times. After that, we utilized five diverse smartphones to capture images of the experimental outcomes, aiming to improve the robustness and adaptability of the YOLOv5 model. Finally, a total of 750 images (30 samples × 5 repetitions × 5 smartphones) were obtained. Moreover, to directly target the test zone, we annotated the constructed dataset using the open-source tool LabelImg. In the dataset, 70% was allocated for training purposes, while 20% was designated for testing, and the remaining 10% was reserved for validating the generalizability of the DL model. This allocation also facilitated the fine-tuning of hyperparameters and mitigated the risk of overfitting.

## III. Results And Discussion

### *A. Results of detecting artificial plasma sample*

In order to assess the practicality of our device in detecting AD biomarkers, we conducted an automated sandwich c-ELISA on our μPAD, with the targeting of detecting Aβ 1-42 peptide in artificial plasma. Four different concentrations were detected (N=5), along with 10-fold dilutions ranging from 1 pg/mL to 1000 pg/mL. The negative control utilized in the experiment consisted of artificial plasma devoid of Aβ 1-42 peptide (0 pg/mL). We collected images of the test zone with a smartphone after every assay. Using ImageJ, we measured the mean grayscale intensity of all test zones. The resulting intensity data was then fitted with Origin software (OriginLab, U.S.A.) using Hill's equation (Fig. 4). The limit of detection was determined to be 15.07 pg/mL, with a coefficient of determination ($R^2$) of 0.995.

In addition, 30 artificial plasma samples for randomized Aβ 1-42 peptide concentration testing were performed. The

Authorized licensed use limited to: Michigan State University. Downloaded on December 23,2024 at 20:18:04 UTC from IEEE Xplore. Restrictions apply.

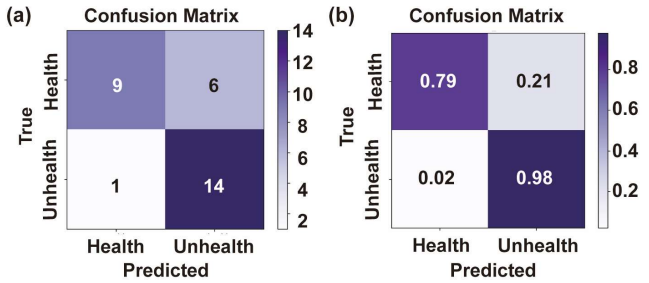


Fig. 5. The confusion matrix of (a) conventional method. (b) YOLOv5 model.

prepared test samples consisted of 15 healthy and 15 unhealthy samples. The purpose of the test was to examine the detection accuracy of the conventional analysis method, which involved manual analysis using ImageJ. According to Fig. 5(a), the outcomes from the conventional analysis method revealed that 6 of the 15 healthy samples were identified as unhealthy samples, exhibiting concentrations surpassing the plasma Aβ 1-42 concentration cut-off value of 16.42 pg/mL [5]. At the same time, 1 of the 15 unhealthy samples with results below the critical value was identified as healthy. Therefore, the accuracy using the conventional analytical method was 76.67% ((9 healthy samples detected + 14 unhealthy samples detected)/30 total samples).

### B. *The training results of the YOLOv5 model*

The true positive (TP) in this work refers to our smartphone-based μPAD's accurate prediction of a positive classification (health, with a value of 0.79 for the sample). The sensor misidentifies a negative sample (unhealthy) as positive (healthy), which is known as a false positive (FP) (the value is 0.02). The values of the true negative (TN) and false negative (FN) are 0.98 and 0.21, respectively, as shown in Fig. 5(b).

The YOLOv5 model's performance is thoroughly assessed with regard to precision, recall, accuracy, specificity, and sensitivity. In general, precision is used to indicate the proportion of positive samples that are classified as positive and can be expressed as (1). Recall quantifies the number of correctly predicted TP cases. It corresponds to the sensitivity of the detection model and can be denoted as (2). During the prediction phase, accuracy is used to measure the accuracy of the categorization model. It represents the percentage of samples that the model correctly predicted in relation to the total number of samples (3). The classification ability of the model improves with increasing accuracy. Specificity refers to the capability of the classification model to accurately predict samples categorized as negative (TN samples). It is expressed as (4) and measures the model's accuracy in identifying samples that belong to the negative class. All these values can be found in Table 1.

$$Precision = \frac{TP}{TP + FP} \tag{1}$$

$$Recall = Sensitivity = \frac{TP}{TP + FN} \tag{2}$$

$$Accuracy = \frac{TP + TN}{TP + FP + TN + FN} \tag{3}$$

$$Specificity = \frac{TN}{FP + TN} \tag{4}$$

TABLE I. THE PERFORMANCE OF THE YOLOV5 MODEL.

| YOLOv5 | Model Performance | | | | |
|---|---|---|---|---|---|
| | *Accuracy* | *Sensitivity* | *Specificity* | *Health accuracy* | *Unhealth accuracy* |
| Value (%) | 88.5% | 79% | 98% | 79% | 98% |

### C. *Android application*

In this work, we developed an Android application featuring a straightforward user interface. The program links to a microcontroller through Bluetooth to adjust the servo motor rotation and conducts image processing and result analysis automatically. After the user logs in, the smartphone connects to the Arduino board via Bluetooth. Subsequently, the user can select the desired type of detection and proceed with sandwich c-ELISA automatically according to the preset procedure. Finally, the detection results will be displayed and saved on the smartphone, indicating whether the sample is healthy or unhealthy.

## IV. CONCLUSION

In this paper, we introduce a fully automated μPAD, controlled by a smartphone enhanced with DL, for accurate offline detection of AD biomarkers (Aβ 1-42). We first created 30 Aβ 1-42 artificial plasma samples, 15 of which represented healthy and 15 of which represented unhealthy ones, in order to provide a dataset for training the DL network. For every sample, we repeated the detection five times, employing five diverse smartphones to capture the results (750 result images). This approach aims to increase the DL algorithm's robustness and adaptability. Subsequently, the dataset was trained with the DL YOLOv5 model, which achieved an accuracy of 88.5%, surpassing the conventional curve-fitting result analysis approach by 11.83%. Ultimately, we directly implemented the DL YOLOv5 model on smartphones for offline detection using Tencent's NCNN framework. In addition, we developed a smartphone application with a user-friendly interface to operate the entire detection process. The distinctive characteristics of our design amplify the advantages of μPAD, making it more suitable for widespread application in resource-limited areas. This offers opportunities for advancing POCT. Simultaneously, it offers a practical method for the detection of AD biomarkers.

## REFERENCES

[1] L. Mosconi *et al.*, "Early detection of Alzheimer's disease using neuroimaging," *Experimental gerontology,* vol. 42, no. 1-2, pp. 129-138, 2007.

[2] M. Sjögren, N. Andreasen, and K. Blennow, "Advances in the detection of Alzheimer's disease—use of cerebrospinal fluid biomarkers," *Clinica Chimica Acta,* vol. 332, no. 1-2, pp. 1-10, 2003.

[3] J. Dukart *et al.*, "Meta-analysis based SVM classification enables accurate detection of Alzheimer's disease across different clinical centers using FDG-PET and MRI," *Psychiatry Research: Neuroimaging,* vol. 212, no. 3, pp. 230-236, 2013.

Authorized licensed use limited to: Michigan State University. Downloaded on December 23,2024 at 20:18:04 UTC from IEEE Xplore. Restrictions apply.

[4] C. Laske *et al.*, "Innovative diagnostic tools for early detection of Alzheimer's disease," *Alzheimer's & Dementia*, vol. 11, no. 5, pp. 561-578, 2015.

[5] H. Fu *et al.*, "A paper-based microfluidic platform with shape-memory-polymer-actuated fluid valves for automated multi-step immunoassays," *Microsystems & nanoengineering,* vol. 5, no. 1, p. 50, 2019.

[6] S. Ghosh *et al.*, "A new microchannel capillary flow assay (MCFA) platform with lyophilized chemiluminescence reagents for a smartphone-based POCT detecting malaria," *Microsystems & Nanoengineering,* vol. 6, no. 1, p. 5, 2020.

[7] W. Yuan *et al.*, "A SERS nanocellulose-paper-based analytical device for ultrasensitive detection of Alzheimer's disease," *Analytica Chimica Acta*, vol. 1301, p. 342447, 2024.

[8] S.-Y. Yang *et al.*, "Detection of plasma biomarkers using immunomagnetic reduction: a promising method for the early diagnosis of Alzheimer's disease," *Neurology and therapy,* vol. 6, pp. 37-56, 2017.

[9] C. E. Teunissen *et al.*, "Plasma amyloid-β (Aβ 42) correlates with cerebrospinal fluid Aβ 42 in Alzheimer's disease," *Journal of Alzheimer's Disease,* vol. 62, no. 4, pp. 1857-1863, 2018.

[10] T. Tian *et al.*, "Integration of target responsive hydrogel with cascaded enzymatic reactions and microfluidic paper-based analytic devices (μPADs) for point-of-care testing (POCT)," *Biosensors and Bioelectronics,* vol. 77, pp. 537-542, 2016.

[11] X. Li *et al.*, "Enhancing the performance of paper-based electrochemical impedance spectroscopy nanobiosensors: An experimental approach," *Biosensors and Bioelectronics,* vol. 177, p. 112672, 2021.

[12] S. Duan *et al.*, "Deep learning-assisted ultra-accurate smartphone testing of paper-based colorimetric ELISA assays," *Analytica Chimica Acta,* vol. 1248, p. 340868, 2023.

[13] T. Cai *et al.*, "A Paper-Based Microfluidic Analytical Device with A Highly Integrated On-Chip Valve For Autonomous ELISA," in *2022 IEEE 35th International Conference on Micro Electro Mechanical Systems Conference (MEMS)*, 2022: IEEE, pp. 271-274.

[14] W.-H. Sung *et al.*, "Paper-Based Detection Device for Alzheimer's Disease—Detecting β-amyloid Peptides (1–42) in Human Plasma," *Diagnostics*, vol. 10, no. 5, p. 272, 2020.

[15] J. Liu *et al.*, "Point-of-care testing based on smartphone: The current state-of-the-art (2017–2018)," *Biosensors and Bioelectronics,* vol. 132, pp. 17-37, 2019.

[16] A. Kumar *et al.*, "Machine learning assisted and smartphone integrated homogeneous electrochemiluminescence biosensor platform for sample to answer detection of various human metabolites," *Biosensors and Bioelectronics,* vol. 238, p. 115582, 2023.

[17] S. Duan *et al.*, "Automatic offline-capable smartphone paper-based microfluidic device for efficient biomarker detection of Alzheimer's disease," *Analytica Chimica Acta,* vol. 1308, p. 342575, 2024.

[18] J. Zhang *et al.*, "Deep Learning for Microfluidic-Assisted *Caenorhabditis elegans* Multi-Parameter Identification Using YOLOv7," *Micromachines,* vol. 14, no. 7, p. 1339, 2023.

[19] H. Zhang *et al.*, "Inkjet printed microfluidic paper-based analytical device (μPAD) for glucose colorimetric detection in artificial urine," *Biomedical microdevices*, vol. 21, p. 48, 2019.

[20] Y. Chen *et al.*, "A dual-readout chemiluminescent-gold lateral flow test for multiplex and ultrasensitive detection of disease biomarkers in real samples," *Nanoscale*, vol. 8, pp. 15205-15212, 2016.

Authorized licensed use limited to: Michigan State University. Downloaded on December 23,2024 at 20:18:04 UTC from IEEE Xplore. Restrictions apply.